Pergamon

SCIENCE DIRECT®

Bioorganic & Medicinal Chemistry 11 (2003) 5101–5116

BIOORGANIC & MEDICINAL CHEMISTRY

Use of Classical and 3-D QSAR to Examine the Hydration State of Juvenile Hormone Esterase Inhibitors

Craig E. Wheelock,[a,b,†] Yoshiaki Nakagawa,[a,*,†] Miki Akamatsu[c] and Bruce D. Hammock[b]

[a]*Division of Applied Life Sciences, Graduate School of Agriculture, Kyoto University, Kyoto 606-8502, Japan*
[b]*Department of Entomology and Cancer Research Center, University of California, Davis, CA 95616, USA*
[c]*Division of Environmental Science and Technology, Graduate School of Agriculture, Kyoto University, Kyoto 606-8502, Japan*

Received 9 May 2003; accepted 20 August 2003

Abstract—Carboxylesterases are important enzymes in the metabolism of numerous pharmaceuticals and agrochemicals. They are of importance in many detoxification pathways, but their endogenous role remains unclear. The most potent esterase inhibitors found to date are trifluoromethylketone (TFK) containing compounds, which have been shown to inhibit both mammalian and insect esterases at the low nM level. The detailed mechanism by which these compounds inhibit the enzyme is still unclear. They are highly hydrated in aqueous solutions, but their mechanism of inhibition suggests that inhibition occurs through the ketone, not the hydrated *gem*-diol. Some studies have stated that the ketone is the inhibitor, while others have reported the *gem*-diol as the active form. Using juvenile hormone esterase (JHE) as a model system, we examined this question using both classical QSAR and 3-D QSAR with comparative molecular field analysis (CoMFA). Classical QSAR analyses demonstrated the high dependence of inhibitor potency upon log P as well as the limitations of sterically unfavorable substituents. The ketone form of the inhibitor consistently provided improved correlations over the *gem*-diol, with the final equations describing 72 and 69% of inhibitor activity, respectively, for 97 compounds. Initial CoMFA analyses for the ketone provided a significant equation for 108 compounds ($q^2=0.412$, $m=6$); however all cross-validated values for the *gem*-diol form of the inhibitors were not statistically significant ($q^2<0.3$). Inclusion of hydrophobicity descriptors in both CoMFA equations increased their significance; however the final ketone equation ($q^2=0.500$, $m=7$) was still statistically improved over the *gem*-diol ($q^2=0.506$, $m=8$). These results support those obtained for the classical QSAR analysis and further illustrate the importance of log P in the inhibition mechanism of these inhibitors. The CoMFA models also identified novel target areas for the synthesis of new JHE inhibitors. These results suggest that the ketone is the active form of TFK-containing inhibitors.

Introduction

Carboxylesterases (EC 3.1.1.1) are a group of enzymes involved in the hydrolysis of ester-containing compounds. They are members of the α/β hydrolase superfamily composed of a characteristic core of 8 β sheets connected by α helices.[1] These enzymes are important in the metabolism of many agrochemicals and pharamaceuticals and have been used to design both prodrugs and softdrugs.[2,3] Carboxylesterases reduce pesticide toxicity by hydrolyzing pyrethroids[4] and binding stoichiometrically to organophosphates[5] and carbamates.[6] While the importance of esterases in metabolizing exogenous esters has been established, the physiological role of esterases is not well understood with the exception of acetylcholinesterase[7] and juvenile hormone esterase (JHE).[8] Mechanistic information derived from the study of JHE can be applied to other esterases and aid in the determination of their endogenous role(s).

JHE is a member of the carboxylesterase family that hydrolyzes the stable α/β unsaturated methyl ester of juvenile hormone (JH) to the corresponding carboxylic acid.[8] JHE regulates JH titer in lepidopteran insects (moths and butterflies), thereby controlling metamorphosis and development.[9] It has been demonstrated that the events leading to pupation are initiated by a reduction in JH titer in the hemolymph.[10] It has therefore been suggested that this enzyme be targeted for use in

*Corresponding author. Tel.: +81-75-753-6117; fax: +81-75-753-6123; e-mail: naka@kais.kyoto-u.ac.jp
†These authors contributed equally to this manuscript.

0968-0896/$ - see front matter © 2003 Elsevier Ltd. All rights reserved.
doi:10.1016/j.bmc.2003.08.023

insect control.[11] JHE represents a biochemical target that is not present in many non-target species (e.g., mammals and fish). Thomas developed a JHE homology model to serve as a predictive basis for the design of biopesticides,[11] and Székács examined the quantitative structure–activity relationship (QSAR) of JHE inhibition to determine the physical parameters necessary for inhibition.[12]

Potent and specific inhibitors are an important tool in the identification of enzyme function.[13] By successfully blocking an enzymatic pathway, information can be inferred about the physiological function of the enzyme.[14] The most potent group of JHE inhibitors identified to date contain a trifluoromethylketone (TFK), consisting of a highly polarized carbonyl moiety (Fig. 1).[9] TFKs have been used to inhibit acetylcholinesterase[15] and other carboxylesterases[16] as well as numerous other enzymes including HIV-1 protease,[17] fatty acid amide hydrolase,[18] and elastase.[19] Extensive classical QSAR analyses have been performed on these compounds by Székács (and references therein).[12] Linderman explored the importance of the unsaturation[20] and steric effects[21] in inhibitor specificity and Roe examined the role of JH mimicry.[22]

The mechanism of substrate hydrolysis is well understood and the catalytic triad has been identified through site-directed mutagenesis.[23] However, the inhibition mechanism by TFKs is less understood. Recent studies have postulated a mechanism for the observed trend in inhibitor potency based upon the hydration extent of the TFK moiety,[24] based on earlier work by Linderman.[25] These studies have provided strong evidence of the inhibition mechanism; however the geometry of the active form of the inhibitor required for esterase inhibition is still unclear. Figure 2 shows a possible mechanism for enzyme inhibition by the two different hydration states (ketone or *gem*-diol). Many researchers have proposed that the ketone is the active form, but this has not yet been conclusively shown. Given that TFKs are transition state analogue inhibitors (TSA), it is logical that the hydrated ketone (consisting of sp^3 hybridized tetrahedral geometry) would be the active inhibitor. This form most accurately mimics the enzyme transition state complex. However, mechanistically it is hard to envision a nucleophilic attack by the catalytic serine residue on a sp^3 carbon. The sp^2 hybridized triganol planar ketone, with it highly polarized electrophilic carbon atom, is a logical site of nuclophilic attack. Various published studies on TFK inhibitors have reported that either the ketone[24,26,27] or the *gem*-diol[28–30] is the active form. This study has therefore examined both the classical and 3-D QSAR of a series of JHE inhibitors and compared the results for the ketone and *gem*-diol forms of the inhibitors as a method to determine the active form of the inhibitor. The results of the two QSAR studies were compared to determine which form of the inhibitor provided the highest level of correlation with biological activity. We propose that the model with the best correlation values is suggestive of the geometry of the active inhibitor.

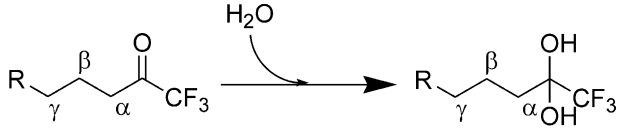

Figure 1. Structure of trifluoromethylketone (TFK) inhibitors showing both the ketone and the hydrated state (*gem*-diol). Greek letters refer to atom positioning relative to the carbonyl or *gem*-diol carbon.

QSAR Methods and Study Design

Classical QSAR

Analyses were performed using QREG2.05.[31] Molecular hydrophobicity was calculated using MacLogP 4.0.[32] Hammett σ values were used for the electronic substituent parameters, which were cited from literature values.[33] In all equations, *n* is the number of compounds used for the regression analyses, *s* is the standard deviation, *r* is the correlation coefficient, and the values in parentheses are 95% confidence intervals. The complete list of inhibitors used in this study is shown in Tables 1–6 with the structural key provided in Figure 3.

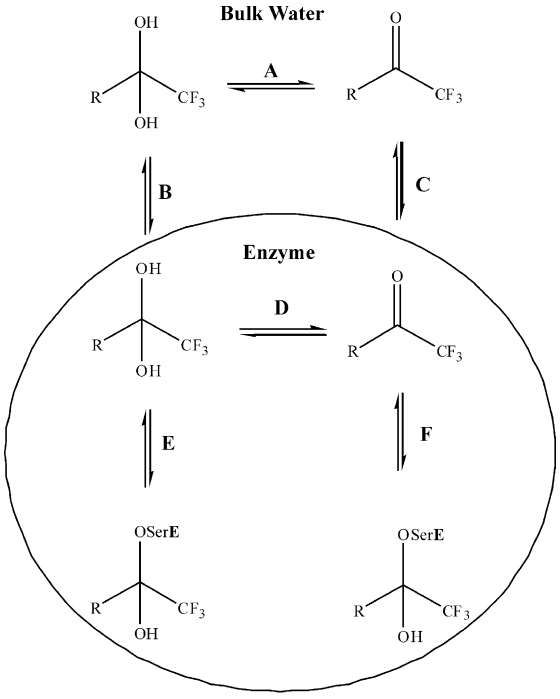

Figure 2. Potential mechanisms for enzyme inhibition by various hydration states of the trifluoromethylketone (TFK) inhibitors. Equilibrium **A** is for the hydration of the inhibitor in bulk water surrounding the enzyme. Equilibrium **B** and **C** are for diffusion of the inhibitor in either the *gem*-diol or ketone form, respectively, into the enzyme. Equilibrium **D** is for the hydration or dehydration of the inhibitor inside the enzyme pocket. Equilibrium **E** and **F** are for the binding of the two different inhibitor states, *gem*-diol and ketone, respectively, to the nucleophilic hydroxyl group on the catalytic serine residue (O-Ser) in the enzyme active site (**E**). The R moiety refers to a range of substituents as shown in Tables 1–6.

Table 1. Activity of alkane, alkene, alkyne and phenyl analogues (pIC_{50}) and their ClogP values

No.	Key[a]	Structure	Obsvd[b]	Eq 7A	Eq 7B	Eq 7A	Eq 7B	Ketone	*Gem*-diol
				Calcd[c]	Calcd[d]	Dev[e]	Dev[f]	ClogP[g]	ClogP[h]
1	**I**	*n*-C_6H_{13}	3.66	4.48	4.68	−0.82	−1.02	3.00	2.65
2	**I**	*n*-C_7H_{15}	4.17	4.94	5.09	−0.77	−0.92	3.53	3.18
3	**I**	*n*-C_8H_{17}	5.17	5.31	5.42	−0.14	−0.25	4.05	3.71
4	**I**	*n*-$C_{10}H_{21}$	6.66	5.82	5.84	0.84	0.82	5.11	4.76
5	**I**	*n*-$C_{12}H_{25}$	7.00	5.99	5.97	1.01	1.03	6.17	5.82
6	**I**	*n*-$C_{13}H_{27}$	5.41	5.96	5.92	−0.55	−0.51	6.70	6.35
7	**I**	*n*-$C_{14}H_{29}$	5.14	5.83	5.79	−0.69	−0.65	7.23	6.88
8	**I**	*n*-$C_{17}H_{35}$	4.85	4.96	4.97	−0.11	−0.12	8.82	8.47
9	**I**	Ph	3.04	3.56	3.42	−0.52	−0.38	2.15	1.39
10	**I**	Ph(4-OMe)	4.15	3.80	3.33	0.35	0.82	2.36	1.31
11	**XVI**	Figure 3	6.52	5.91	5.82	0.61	0.70	5.44	4.69
12	**XII**	Figure 3	6.70	5.92	5.95	0.78	0.75	6.88	6.13
13	**XIV**	Figure 3	3.30[i]	5.18	5.03	−1.88	−1.73	3.85	3.10
14	**II**	*E*-*n*-C_6H_{13}	5.14	5.36	5.57	−0.22	−0.43	4.12	4.02
15	**II**	*Z*-*n*-C_6H_{13}	4.10[i]	5.36	5.57	−1.26	−1.47	4.12	4.02
16	**II**	*E*-*n*-C_8H_{17}	6.06	5.84	5.91	0.22	0.15	5.18	5.08
17	**III**	*n*-C_4H_9	5.49	5.11	6.76	0.38	−1.27	1.94	3.09
18	**III**	*n*-C_6H_{13}	6.40	6.29	7.37	0.12	−0.97	3.00	4.15
19	**III**	*n*-C_8H_{17}	7.24	7.12	7.67	0.12	−0.43	4.05	5.21
20	**III**	*n*-$C_{10}H_{21}$	7.57	7.63	7.67	−0.06	−0.10	5.11	6.26
21	**III**	*n*-$C_{12}H_{25}$	8.00	7.80	7.37	0.20	0.63	6.17	7.32
22	**III**	Ph	5.27	5.57	4.92	−0.30	0.35	2.32	1.19

[a]Structure key as described in Figure 3.
[b]Observed pIC_{50} values taken from Székács.[12]
[c]Calculated pIC_{50} values for ketone inhibitors using eq 7A.
[d]Calculated pIC_{50} values for *gem*-diol inhibitors using eq 7B.
[e]Deviation in ketone inhibitor pIC_{50} values calculated with eq 7A from observed values.
[f]Deviation in *gem*-diol inhibitor pIC_{50} values calculated with eq 7B from observed values.
[g]Calculated log P (ClogP) values for ketone inhibitors.[32]
[h]Calculated log P (ClogP) values for *gem*-diol inhibitors.[32]
[i]Not included in the analyses.

Comparative molecular field analysis (CoMFA) procedure

All computations were performed with the molecular modeling software package SYBYL ver. 6.8 (Tripos Co., St. Louis, MO, USA). CoMFA studies were initiated by downloading the X-ray crystallographic coordinates of 1,1,1-trifluoro-3-(octane-1-sulfonyl)-propane-2,2-diol (**101**) and 1,1,1-trifluoro-5-phenyl-4-thiapentane-2,2-diol (**50**) from the Cambridge Crystallographic Data Centre (Deposition Number 'CCDC 178195'[24] and 'FORFUN',[34] respectively). Molecules **1**–**49** and **96**–**109** were constructed from compound **101** and molecules **51**–**95** were constructed from compound **50**. Both crystal structures showed the ligand in its hydrated (*gem*-diol) form. This form was subsequently used for all hydrated compounds, however for ketone-containing inhibitors; the *gem*-diol was converted to the ketone using the SYBYL drawing module. Structures were subsequently replaced with the appropriate functional group using the drawing module to generate all compounds reported in this work. After structure generation, the geometry of all molecules was fully optimized using PM3 and charges were calculated with AM1. CoMFA superpositions were performed using the selected atoms shown in Figure 4. These atoms were chosen for superposition based upon the currently accepted mechanism for esterase inhibition.[2] Additionally, any attempts to include additional atoms (i.e., atoms beyond the α position) were incompatible with the Sybyl program due to molecule heterogeneity. We therefore chose atoms that were common to all 109 compounds.

The analyses were conducted using the SYBYL QSAR module. The lattice spacing was 2 Å, and a +1 charge and a sp^3 carbon were used as probes to estimate the electrostatic and steric molecular fields, respectively. The molecules were superposed in the lattice space of 18 Å × 24 Å × 21 Å ($X=-9$ to 9, $Y=-12$ to 12, $Z=-10$ to 11). The electrostatic and steric potential energies at each lattice point were calculated using Coulombic and Lennard–Jones potential functions, respectively. The hydrophobic effect was evaluated using log P as the lattice-independent external descriptor. The correlations of the biological activity index with the lattice variables and log P and $(\log P)^2$ were also analyzed with the partial least squares (PLS) method. We initially selected the number of components in the set from the cross-validation (the leave-one-out method) setting the column filtering at 2 kcal/mol, and then performed the analysis using the optimum number of latent variables which was deduced from the cross-validation tests without actual cross-validation. The CoMFA results were represented by the leave-one-out cross-validated correlation coefficient, q, the sum-of-squares deviation, SD, the number of components, m, the conventional correlation coefficient, r, and the standard deviation, s, in addition to the relative contribution (%) of descriptors to the correlation equation. The results

Table 2. Activity of sulfide analogues (pIC_{50}) and their ClogP values

No.	Key[a]	Structure	Obsvd[b]	Eq 7A	Eq 7B	Eq 7A	Eq 7B	Ketone	*Gem*-diol
				Calcd[c]	Calcd[d]	Dev[e]	Dev[f]	ClogP[g]	ClogP[h]
23	**IV**	*n*-C_4H_9	5.82	5.66	5.66	0.16	0.16	2.40	1.84
24	**IV**	*n*-C_5H_{11}	6.11	6.22	6.18	−0.11	−0.07	2.93	2.37
25	**IV**	*n*-$(CH_3)_3C$	5.30	5.24	5.27	0.06	0.03	2.05	1.49
26	**IV**	2-Me-Butyl-	5.80	6.09	6.06	−0.29	−0.26	2.80	2.24
27	**IV**	3-Me-Butyl-	5.60	6.09	6.06	−0.49	−0.46	2.80	2.24
28	**IV**	*n*-C_6H_{13}	7.51	6.69	6.62	0.82	0.89	3.46	2.90
29	**IV**	*n*-C_7H_{15}	8.09	7.08	6.99	1.01	1.10	3.99	3.43
30	**IV**	*n*-C_8H_{17}	8.62	7.38	7.28	1.24	1.34	4.51	3.96
31	**IV**	2,4,4-Me-C_8H_{14}	7.98	7.77	7.66	0.21	0.32	5.71	5.15
32	**IV**	*n*-C_9H_{19}	8.43	7.61	7.50	0.82	0.94	5.04	4.49
33	**IV**	*n*-$C_7H_{15}CH(CH_3)$	9.77[i]	7.52	7.41	2.25	2.36	4.82	4.27
34	**IV**	*n*-$C_{10}H_{21}$	7.70	7.75	7.64	−0.05	0.07	5.57	5.02
35	**IV**	*n*-$C_7H_{15}CH(Et)$	8.24	7.70	7.59	0.54	0.65	5.35	4.80
36	**IV**	*n*-$C_{11}H_{23}$	7.37	7.80	7.70	−0.43	−0.33	6.10	5.54
37	**IV**	*n*-$C_7H_{15}CH$(*n*-Pr)	7.89	7.79	7.68	0.10	0.21	5.88	5.32
38	**IV**	*n*-$C_{12}H_{25}$	7.82	7.77	7.69	0.05	0.13	6.63	6.07
39	**IV**	*n*-$C_7H_{15}CH$(*n*-Bu)	7.16	7.80	7.70	−0.64	−0.54	6.41	5.85
40	**IV**	*n*-$C_{13}H_{27}$	7.35	7.66	7.61	−0.31	−0.26	7.16	6.60
41	**IV**	*n*-$C_{14}H_{29}$	6.40	7.47	7.44	−1.07	−1.04	7.69	7.13
42	**IV**	*n*-$C_{16}H_{33}$	6.20	6.82	6.90	−0.62	−0.70	8.75	8.19
43	**IV**	*n*-$C_{18}H_{37}$	6.30	5.85	6.05	0.45	0.26	9.80	9.25
44	**IV**	Cyclopentyl	5.01	5.52	5.54	−0.51	−0.53	2.28	1.73
45	**IV**	Cyclohexyl	5.28	6.13	6.10	−0.85	−0.82	2.84	2.29
46	**XI**	Figure 3	8.35[i]	7.53	7.41	0.82	0.94	4.83	4.27
47	**XV**	Figure 3	8.12[i]	6.86	6.78	1.26	1.34	3.68	3.12
48	**XIII**	Figure 3	8.51[i]	7.54	7.43	0.97	1.08	4.87	4.32
49	**X**	Figure 3	8.49[i]	6.90	6.82	1.59	1.68	3.73	3.17

[a]Structure key as described in Figure 3.
[b]Observed pIC_{50} values taken from Székács.[12]
[c]Calculated pIC_{50} values for ketone inhibitors using eq 7A.
[d]Calculated pIC_{50} values for *gem*-diol inhibitors using eq 7B.
[e]Deviation in ketone inhibitor pIC_{50} values calculated with eq 7A from observed values.
[f]Deviation in *gem*-diol inhibitor pIC_{50} values calculated with eq 7B from observed values.
[g]Calculated log P (ClogP) values for ketone inhibitors.[32]
[h]Calculated log P (ClogP) values for *gem*-diol inhibitors.[32]
[i]Not included in the analyses.

were visualized by contour maps using connected lattice points having an equivalent coefficient level for each molecular field surrounding a set of superposed molecules.

Results

We developed both classical and 3-D QSAR models for the set of TFK inhibitors described by Székács.[12] These two models were compared in terms of their ability to predict the inhibition potency of the range of compounds analyzed in this study as well as their ability to describe the structure activity relationship with the highest level of correlation using the least number of parameters. Log P values were calculated for both the ketone and *gem*-diol forms of all inhibitors listed in Tables 1–6 and used to generate the following equations. The results for the QSAR analyses are presented for both the ketone and *gem*-diol analogues. In all cases, the first equation (A) is for the ketone and the second (1B) is for the *gem*-diol. In no instance did the *gem*-diol equations prove to be statistically superior to those provided by the ketone. The results for the classical and 3-D QSAR are each described separately in the following sections.

Classical QSAR

We began building the QSAR model with a series of saturated aliphatic compounds (Table 1). Although the number of compounds is extremely small, thus making statistical interpretation difficult, the following parabolic relationship was derived:

$$\begin{aligned} pIC_{50} =& 3.114(\pm 2.357)\log P - 0.253(\pm 0.202) \\ & \times (\log P)^2 \\ & - 3.350(\pm 6.342) \qquad (1A) \\ n = 8 \quad & s = 0.716 \quad r^2 = 0.714 \\ F(2,5) = 6.229 \quad & p < 0.05 \quad \log P_{opt} = 6.15 \end{aligned}$$

$$\begin{aligned} pIC_{50} =& 2.937(\pm 2.216)\log P - 0.253(\pm 0.202) \\ & \times (\log P)^2 \\ & - 2.294(\pm 5.558) \qquad (1B) \\ n = 8 \quad & s = 0.716 \quad r^2 = 0.714 \\ F(2,5) = 6.232 \quad & p < 0.05 \quad \log P_{opt} = 5.80 \end{aligned}$$

These two equations are essentially identical, showing no statistical difference between the *gem*-diol and ketone

Table 3. Activity of substituted phenyl sulfide analogues (pIC_{50}) and their ClogP values

No.	Key[a]	Structure	Obsvd[b]	Eq 7A	Eq 7B	Eq 7A	Eq 7B	Eq 9	Eq 9	Ketone	*Gem*-diol
				Calcd[c]	Calcd[d]	Dev[e]	Dev[f]	Calcd[g]	Dev[h]	ClogP[i]	ClogP[j]
50	V	H	5.06	5.69	5.72	−0.63	−0.66	5.64	−0.58	2.43	1.92
51	V	2-Cl	5.68	6.47	6.44	−0.79	−0.76	6.26	−0.58	3.20	2.67
52	V	2-Br	6.17	6.60	6.56	−0.43	−0.39	6.41	−0.24	3.35	2.82
53	V	2-Me	5.37	6.22	6.20	−0.85	−0.83	6.26	−0.89	2.93	2.40
54	V	2-Et	5.54	6.69	6.64	−1.15	−1.10	6.77	−1.23	3.46	2.93
55	V	2-*i*Pr	6.47	6.99	6.92	−0.52	−0.45	7.17	−0.70	3.86	3.33
56	V	2-OMe	5.70	5.16	5.23	0.54	0.47	5.38	0.33	1.98	1.45
57	V	2-CH_2OH	5.15	4.36	4.50	0.79	0.65	4.61	0.55	1.39	0.86
58	V	2-OPh	6.66	7.17	7.09	−0.51	−0.43	7.36	−0.70	4.13	3.60
59	V	2-NHPh	7.52	7.03	6.96	0.49	0.57	7.39	0.13	3.91	3.38
60	V	3-Cl	6.40	6.47	6.44	−0.07	−0.04	6.17	0.24	3.20	2.67
61	V	3-Br	6.06	6.60	6.56	−0.54	−0.50	6.30	−0.24	3.35	2.82
62	V	3-CF_3	5.60	6.65	6.60	−1.05	−1.00	6.33	−0.73	3.41	2.88
63	V	3-Me	6.89	6.22	6.20	0.67	0.69	6.19	0.70	2.93	2.40
64	V	3-OMe	5.89	5.64	5.67	0.25	0.22	5.51	0.38	2.38	1.85
65	V	4-F	5.08	5.91	5.92	−0.83	−0.84	5.80	−0.72	2.63	2.10
66	V	4-Cl	5.89	6.47	6.44	−0.58	−0.55	6.26	−0.37	3.20	2.67
67	V	4-Br	6.39	6.60	6.56	−0.21	−0.17	6.41	−0.02	3.35	2.82
68	V	4-Me	6.96	6.22	6.20	0.74	0.76	6.26	0.70	2.93	2.40
69	V	4-*t*Bu	8.12	7.24	7.16	0.88	0.96	7.60	0.52	4.25	3.73
70	V	4-OH	5.21	4.87	4.97	0.34	0.25	5.22	−0.01	1.76	1.23
71	V	4-OMe	5.89	5.64	5.67	0.25	0.22	5.78	0.12	2.38	1.85
72	V	4-$(CH_3)_2N$–	7.05	5.87	5.89	1.18	1.16	6.36	0.69	2.59	2.07
73	V	2,5-Cl_2	7.64	7.04	6.97	0.60	0.67	6.74	0.90	3.93	3.40
74	V	2,6-Cl_2	7.11	7.04	6.97	0.07	0.14	6.83	0.28	3.93	3.40
75	V	3,4-Cl_2	7.70	6.96	6.89	0.74	0.81	6.62	1.08	3.81	3.28
76	V	2,4-Me_2	6.04	6.67	6.62	−0.63	−0.58	6.87	−0.83	3.43	2.90
77	V	2,5-Me_2	6.77	6.67	6.62	0.10	0.15	6.80	−0.03	3.43	2.90
78	V	2,6-Me_2	6.92	6.67	6.62	0.25	0.30	6.87	0.05	3.43	2.90
79	V	3,4-Me_2	7.96	6.63	6.58	1.33	1.38	6.75	1.21	3.38	2.85
80	V	3,5-Me_2	5.74	6.67	6.62	−0.93	−0.88	6.74	−1.00	3.43	2.90
81	V	2-Me-4-*t*Bu	8.52	7.50	7.40	1.02	1.12	8.19	0.33	4.75	4.23
82	V	3-Me-4-Br	7.89	6.99	6.92	0.90	0.97	6.96	0.94	3.85	3.32
83	V	2,4,5-Cl_3	7.49	7.39	7.30	0.10	0.19	7.19	0.31	4.53	4.00
84	V	2,3,5,6-F_4	5.92	6.23	6.21	−0.31	−0.29	5.62	0.30	2.94	2.41
85	V	2,3,4,5,6-Cl_5	7.80	7.77	7.66	0.03	0.14	7.96	−0.16	5.71	5.19
86	V	2,3,4,5,6-F_5	4.96	6.29	6.28	−1.33	−1.32	5.65	−0.69	3.01	2.49

[a]Structure key as described in Figure 3.
[b]Observed pIC_{50} values taken from Székács.[12]
[c]Calculated pIC_{50} values for ketone inhibitors using eq 7A.
[d]Calculated pIC_{50} values for *gem*-diol inhibitors using eq 7B.
[e]Deviation in ketone inhibitor pIC_{50} values calculated with eq 7A from observed values.
[f]Deviation in *gem*-diol inhibitor pIC_{50} values calculated with eq 7B from observed values.
[g]Calculated pIC_{50} values for inhibitors using eq 9.
[h]Deviation in inhibitor pIC_{50} values calculated with eq 9 from observed values.
[i]Calculated log P (ClogP) values for ketone inhibitors.[32]
[j]Calculated log P (ClogP) values for *gem*-diol inhibitors.[32]

forms of the inhibitor. According to eq 1A, the optimum ketone log P (log P_{opt}) value is estimated to be 6.15, whereas the *gem*-diol optimum is 5.80. These two equations are interesting as they show a rather high optimum log P value for inhibition potency. The optimum log P values are slightly greater than previous studies that have shown optimum log P values for JHE inhibition from approximately 4–5,[12,26] which is very similar to the calculated log P value (ClogP) for JH (4.35).[16] We derived a similar correlation using the calculated molar refractivity (CMR) and its squared term ($s = 0.713$ and $r^2 = 0.716$). This result further demonstrates the high degree of correlation between MR and log P ($r^2 = 1$ between ClogP and CMR for these eight compounds). The inclusion of the $(\log P)^2$ term indicates that there is an optimal value for JHE inhibition, which has been reported by other researchers.[12] Roe also derived a parabolic relationship for a series of TFK inhibitors of JHE using MR values.[22]

We examined the ability of eq. 1 to predict the activity of other inhibitors and found that *para*-substituted phenyl compounds were fairly well predicted. Interestingly, some phenyl compounds containing multiple functional groups were still well-predicted by this simple equation, demonstrating the importance of log P in the biological activity of these compounds. Of particular interest was the fact that olefin analogues with *Z*-geometry were well predicted, while the corresponding *E*-forms were predicted to be an order of magnitude more active than observed values. However, all alkyne analogues (**17**–**22**) were predicted to be two orders of magnitude higher than their observed values using eq. 1. Thus we reanalyzed compounds **1**–**22** by setting an indicator variable I-triple which takes a value of 1 for

Table 4. Activity values of other sulfide compounds (pIC_{50}) and their ClogP values

No.	Key[a]	Structure	Obsvd[b]	Eq 7A Calcd[c]	Eq 7B Calcd[d]	Eq 7A Dev[e]	Eq 7B Dev[f]	Ketone ClogP[g]	*Gem*-diol ClogP[h]
87	**VI**, $n=1$	H	4.82	4.70	4.72	0.12	0.10	2.68	2.15
88	**VI**, $n=1$	2-Cl	5.18	5.37	5.34	−0.19	−0.16	3.39	2.86
89	**VI**, $n=1$	4-Cl	5.34	5.37	5.34	−0.03	−0.00	3.39	2.86
90	**VI**, $n=1$	2-Me	4.90	5.15	5.13	−0.25	−0.23	3.13	2.60
91	**VI**, $n=1$	3-Me	5.10	5.19	5.17	−0.09	−0.07	3.18	2.65
92	**VI**, $n=1$	4-Me	5.20	5.19	5.17	0.01	0.03	3.18	2.65
93	**VI**, $n=1$	4-$C_{12}H_{25}$	5.80	5.36	5.46	0.44	0.35	9.00	8.47
94	**VI**, $n=2$	H	5.49	6.20	6.16	−0.71	−0.67	2.91	2.35
95	**VI**, $n=3$	H	6.77	6.55	6.49	0.22	0.29	3.29	2.73

[a]Structure key as described in Figure 3.
[b]Observed pIC_{50} values taken from Székács.[12]
[c]Calculated pIC_{50} values for ketone inhibitors using eq 7A.
[d]Calculated pIC_{50} values for *gem*-diol inhibitors using eq 7B.
[e]Deviation in ketone inhibitor pIC_{50} values calculated with eq 7A from observed values.
[f]Deviation in *gem*-diol inhibitor pIC_{50} values calculated with eq 7B from observed values.
[g]Calculated log P (ClogP) values for ketone inhibitors.[32]
[h]Calculated log P (ClogP) values for *gem*-diol inhibitors.[32]

alkyne analogues containing a triple bond between the β and γ positions (see Fig. 1 for clarification of bond positioning).

$$\begin{aligned} pIC_{50} =& 2.022(\pm 0.894)\log P - 0.156(\pm 0.087) \\ & \times (\log P)^2 \\ & + 2.205(\pm 0.754)\text{I-triple} - 0.584(\pm 2.143) \quad (2A) \\ n = 22 \quad & s = 0.717 \quad r^2 = 0.776 \\ F(3, 18) = 20.847 \quad & p < 0.001 \quad \log P_{opt} = 6.48 \end{aligned}$$

$$\begin{aligned} pIC_{50} =& 1.271(\pm 0.806)\log P - 0.094(\pm 0.086) \\ & \times (\log P)^2 \\ & + 1.614(\pm 0.835)\text{I-triple} - 1.608(\pm 1.748) \quad (2B) \\ n = 22 \quad & s = 0.829 \quad r^2 = 0.702 \\ F(3, 18) = 14.079 \quad & p < 0.001 \quad \log P_{opt} = 6.76 \end{aligned}$$

Even though the standard error of eq. 2 is very high, 77% of the correlation for the ketone inhibitor was described by log P and an indicator variable I-triple, as opposed to 70% for the *gem*-diol. Compound **13,** which has a terpenoid substructure and was designed as a JH mimic with two epoxide moieties,[20] deviated significantly from eq 2. Additionally, compound **15** containing a *Z* double bond was also poorly predicted. By omitting compounds **13** and **15**, the correlation for 20 compounds listed in Table 1 was improved as shown in eq. 3.

$$\begin{aligned} pIC_{50} =& 2.207(\pm 0.714)\log P - 0.179(\pm 0.070) \\ & \times (\log P)^2 \\ & + 1.967(\pm 0.610)\text{I-triple} - 0.665(\pm 1.690) \quad (3A) \\ n = 20 \quad & s = 0.560 \quad r^2 = 0.852 \\ F(3, 16) = 30.786 \quad & p < 0.001 \quad \log P_{opt} = 6.16 \end{aligned}$$

$$\begin{aligned} pIC_{50} =& 1.394(\pm 0.735)\log P - 0.112(\pm 0.079) \\ & \times (\log P)^2 \\ & + 1.440(\pm 0.765)\text{I-triple} - 1.652(\pm 1.579) \quad (3B) \\ n = 20 \quad & s = 0.739 \quad r^2 = 0.743 \\ F(3, 16) = 15.389 \quad & p < 0.001 \quad \log P_{opt} = 6.22 \end{aligned}$$

While both eqs 3A and 3B are statistically significant, eq. 3A provides a superior correlation, showing a significant difference between the ketone and *gem*-diol forms. We used eq. 3 to analyze a wide variety of sulfide analogues as shown in Tables 2–4. Interestingly, all sulfide analogues (**23**–**95**), containing a S atom β to the TFK moiety, were predicted with eq. 3 to have increased activity relative to observed values. Therefore, we added these compounds to eq. 3 and reanalyzed by setting another indicator variable I-S which takes a value of 1 for sulfide-containing compounds. It was necessary to exclude several compounds from the new eq. 4, including compounds **13** and **15**, which had already been excluded from eq. 3, and compounds **33** and **46**–**49**. These compounds were all designed as specific mimics of JH and contain various groups branching off from the main backbone or multiple sites of unsaturation.[20–22] The structure of these compounds appears to be too complicated to be described by this relatively simple QSAR analysis.

$$\begin{aligned} pIC_{50} =& 2.059(\pm 0.412)\log P - 0.168(\pm 0.039) \\ & \times (\log P)^2 + 1.919(\pm 0.702)\text{I-triple} + 1.707 \\ & \times (\pm 0.430)\text{I} - \text{S} - 0.242(\pm 1.076) \quad (4A) \\ n = 88 \quad & s = 0.714 \quad r^2 = 0.658 \\ F(4, 83) = 39.960 \quad & p < 0.001 \quad \log P_{opt} = 6.13 \end{aligned}$$

Table 5. Activity of sulfoxide and sulfone analogues (pIC_{50}) and their ClogP values

No.	Key[a]	Structure	Obsvd	Eq 7A Calcd[b]	Eq 7B Calcd[c]	Eq 7A Dev[d]	Eq 7B Dev[e]	Ketone ClogP[f]	*Gem*-diol ClogP[g]
96	**VIII**	*n*-C_8H_{17}	7.37[h]	7.19	7.11	0.18	0.26	3.00	2.31
97	**VIII**	Ph	4.21[h]	4.57	4.72	−0.36	−0.51	0.95	0.31
98	**VIII**	Ph(4-*t*Bu)	7.64[h]	6.87	6.95	0.77	0.69	2.77	2.14
99	**IX**	Ph	3.98[h]	4.50	4.66	−0.52	−0.68	0.91	0.27
100	**IX**	*n*-C_6H_{13}	6.83[i]	5.92	5.88	0.91	0.95	1.87	1.17
101	**IX**	*n*-C_8H_{17}	6.90[i]	7.11	7.03	−0.21	−0.13	2.92	2.23
102	**IX**	*n*-$C_{10}H_{21}$	7.36[i]	7.98	7.88	−0.62	−0.52	3.98	3.28
103	**IX**	*n*-$C_{12}H_{25}$	7.21[i]	8.51	8.43	−1.30	−1.22	5.04	4.34
104	**IX**	Ph-C_2H_4	6.31[i]	5.16	5.16	1.15	1.15	1.32	0.62

[a]Structure key as described in Figure 3.
[b]Calculated pIC_{50} values for ketone inhibitors using eq 7A.
[c]Calculated pIC_{50} values for *gem*-diol inhibitors using eq 7B.
[d]Deviation in ketone inhibitor pIC_{50} values calculated with eq 7A from observed values.
[e]Deviation in *gem*-diol inhibitor pIC_{50} values calculated with eq 7B from observed values.
[f]Calculated log P (ClogP) values for ketone inhibitors.[32]
[g]Calculated log P (ClogP) values for *gem*-diol inhibitors.[32]
[h]Observed pIC_{50} values taken from Székács.[12]
[i]Observed pIC_{50} values taken from Kamita.[9]

Table 6. Activity values of branched sulfide analogues (pIC_{50}) and their ClogP values

No.	Key[a]	Structure	Obsvd[b]	Eq 7A Calcd[c]	Eq 7B Calcd[d]	Eq 7A Dev[e]	Eq 7B Dev[f]	Ketone ClogP[g]	*Gem*-diol ClogP[h]
105	**VII**	R = CH_3, R′ = H	9.06	7.61	7.41	1.45	1.65	5.04	4.27
106	**VII**	R = Et, R′ = H	5.32	7.75	7.59	−2.43	−2.27	5.57	4.80
107	**VII**	R = *n*-Pr, R′ = H	4.09	7.80	7.68	−3.71	−3.59	6.10	5.32
108	**VII**	R = Ph, R′ = H	4.09	7.80	7.70	−3.71	−3.61	6.21	5.63
109	**VII**	R = CH_3, R′ = CH_3	8.07	7.70	7.52	0.37	0.55	5.35	4.58

[a]Structure key as described in Figure 3.
[b]Observed pIC_{50} values taken from Székács.[12] All values were not included in the analyses.
[c]Calculated pIC_{50} values for ketone inhibitors using eq 7A.
[d]Calculated pIC_{50} values for *gem*-diol inhibitors using eq 7B.
[e]Deviation in ketone inhibitor pIC_{50} values calculated with eq 7A from observed values.
[f]Deviation in *gem*-diol inhibitor pIC_{50} values calculated with eq 7B from observed values.
[g]Calculated log P (ClogP) values for ketone inhibitors.[32]
[h]Calculated log P (ClogP) values for *gem*-diol inhibitors.[32]

$$\begin{aligned} pIC_{50} =& 1.709(\pm 0.378)\log P - 0.150(\pm 0.039) \\ & \times (\log P)^2 + 1.443(\pm 0.729)\text{I-triple} \\ & + 1.664(\pm 0.452)\text{I-S} + 1.173(\pm 0.904) \qquad (4B) \\ n = 88 \quad & s = 0.751 \quad r^2 = 0.622 \\ F(4, 83) = 34.069 \quad & p < 0.001 \quad \log P_{opt} = 5.70 \end{aligned}$$

Since the I-triple and I-S coefficients are very similar, we combined them as I(T + S) to derive eq. 5.

$$\begin{aligned} pIC_{50} =& 2.060(\pm 0.411)\log P - 0.168(\pm 0.039) \\ & \times (\log P)^2 \\ & + 1.723(\pm 0.426)\text{I}(\text{T} + \text{S}) - 0.243(\pm 1.073) \qquad (5A) \\ n = 88 \quad & s = 0.712 \quad r^2 = 0.656 \\ F(3, 84) = 53.447 \quad & p < 0.001 \quad \log P_{opt} = 6.07 \end{aligned}$$

$$\begin{aligned} pIC_{50} =& 1.701(\pm 0.376)\log P - 0.150(\pm 0.039) \\ & \times (\log P)^2 \\ & + 1.640(\pm 0.446)\text{I}(\text{T} + \text{S}) + 1.201(\pm 0.897) \qquad (5B) \\ n = 88 \quad & s = 0.749 \quad r^2 = 0.619 \\ F(3, 84) = 45.562 \quad & p < 0.001 \quad \log P_{opt} = 5.67 \end{aligned}$$

Eqs 5A and 5B had improved *F*-values over eqs 4A and 4B, while the correlations coefficients remained essentially unchanged. This observation supports the combining of these two variables, which may both describe a form of substituent electron effects. Eq 5A for the ketone provided a slightly improved correlation over 5B for the *gem*-diol; however the difference was not as pronounced as eqs 3A and 3B. The inclusion of sulfur-containing compounds greatly narrowed the difference between the ketone and *gem*-diol equations. All compounds listed in Tables 2 and 3 were fairly well predicted by eq. 5 with the use of only three parameters for the analysis. However, the predicted values of all benzyl analogues

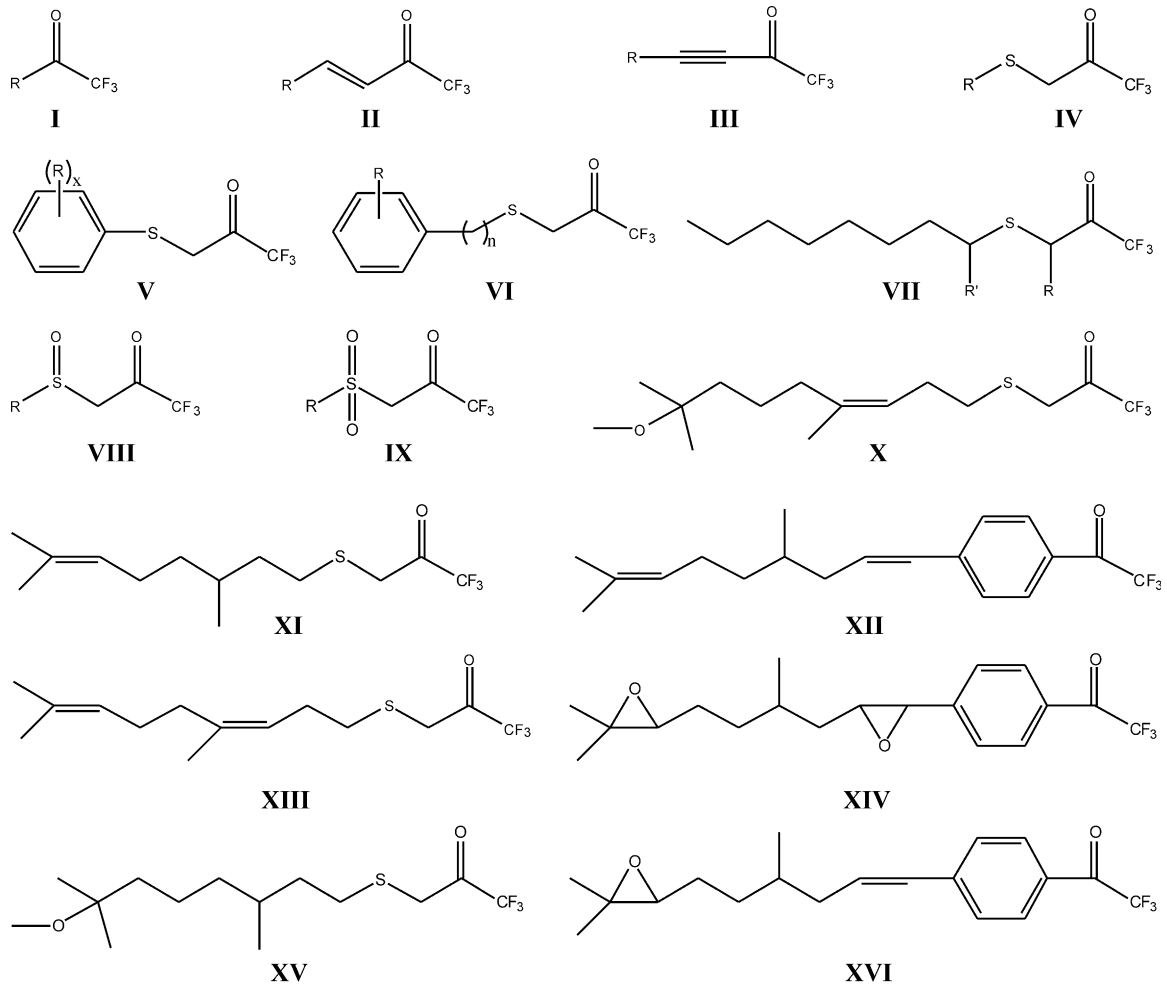

Figure 3. General structures of all trifluoromethylketone (TFK) inhibitors as shown in Tables 1–6. Roman numerals indicate base inhibitor structure and Arabic numerals are used for specific compounds.

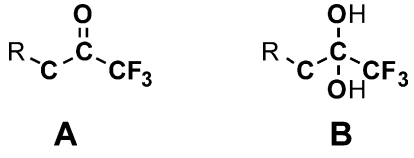

Figure 4. Superposition for CoMFA analysis. Atoms in bold text were chosen for superposition of the ketone (A) or *gem*-diol (B). All hydrogen atoms were excluded from the superposition.

(**87**–**93**) listed in Table 4 were uniformly higher than their observed values, but the phenylethyl (**94**) and phenylpropyl (**95**) analogues were well predicted. Therefore, we used an additional indicator parameter (I-Benzyl) for all benzyl-containing compounds (**87**–**93**) to derive eq. 6.

$$\begin{aligned} \mathrm{pIC_{50}} =& 1.984(\pm 0.364)\mathrm{logP} - 0.161(\pm 0.034) \\ & \times (\mathrm{logP})^2 \\ & + 1.838(\pm 0.379)\mathrm{I(T+S)} \\ & - 1.247(\pm 0.498)\text{I-Benzyl} - 0.078(\pm 0.949) \\ n = 88 \quad & s = 0.628 \quad r^2 = 0.736 \\ F(4, 83) = 57.627 \quad & p < 0.001 \quad \mathrm{logP_{opt}} = 6.16 \end{aligned} \tag{6A}$$

$$\begin{aligned} \mathrm{pIC_{50}} =& 1.635(\pm 0.339)\mathrm{logP} - 0.143(\pm 0.035) \\ & \times (\mathrm{logP})^2 \\ & + 1.753(\pm 0.403)\mathrm{I(T+S)} \\ & - 1.235(\pm 0.533)\text{I-Benzyl} + 1.329(\pm 0.808) \\ n = 88 \quad & s = 0.672 \quad r^2 = 0.697 \\ F(4, 83) = 47.709 \quad & p < 0.001 \quad \mathrm{logP_{opt}} = 5.72 \end{aligned} \tag{6B}$$

The addition of the I-Benzyl term improved both equations. However, the activity of the sulfoxide and sulfone analogues (**96**–**104**) shown in Table 5 were under-predicted by eq. 6. We therefore used another indicator variable I-(S=O), which takes a value of 1 for S(=O) and $S(=O)_2$ compounds, to formulate eq. 7.

$$\begin{aligned} \mathrm{pIC_{50}} =& 1.851(\pm 0.325)\mathrm{logP} - 0.150(\pm 0.031) \\ & \times (\mathrm{logP})^2 \\ & + 1.810(\pm 0.389)\mathrm{I(T+S)} \\ & + 2.713(\pm 0.602)\text{I-(S=O)} \\ & - 1.260(\pm 0.514)\text{I-Benzyl} - 0.269(\pm 0.860) \\ n = 97 \quad & s = 0.649 \quad r^2 = 0.723 \\ F(5, 91) = 47.884 \quad & p < 0.001 \quad \mathrm{logP_{opt}} = 6.17 \end{aligned} \tag{7A}$$

$$\begin{aligned} pIC_{50} =& 1.547(\pm 0.299)\log P - 0.135(\pm 0.032) \\ & \times (\log P)^2 \\ & + 1.736(\pm 0.411)I(T+S) \\ & + 2.722(\pm 0.641)I\text{-}(S{=}O) \\ & - 1.246(\pm 0.543)I\text{-Benzyl} - 1.531(\pm 0.735) \\ n = 97 \quad & s = 0.687 \quad r^2 = 0.691 \\ F(5,91) = 40.763 \quad & p < 0.001 \quad \log P_{opt} = 5.73 \end{aligned} \tag{7B}$$

The addition of the sulfoxide and sulfone compounds did not dramatically affect the difference between the two equations. The *F*-values decreased in both equations and the r^2 values remained almost constant. In the final eq. 7, compounds **13**, **15**, **33**, **46**–**49** were excluded. During the development of the ketone correlation equations, the optimum hydrophobicity value was constant to be 6.19 (±0.13), while the optimal *gem*-diol value was 5.94 (±0.41).

We also attempted to add compounds **105**–**109** (Table 6) containing alkyl or aryl substituents in the α or γ position to eq. 7. However, the biological activity of compounds with a methyl group were greatly under predicted, whereas the inclusion of larger alkyl or ring structures resulted in predicted values that were 300–5000 times higher than observed values. These results were also observed with compound **33** and are in agreement with data reported by Linderman showing narrow steric constraints in the active site of JHE as evidenced by the negative steric effects of substitution either α or α′ to the sulfur.[21] There is a small enhancement of activity with methyl substitution, but larger groups are detrimental to activity. These effects cannot be described by the current QSAR equations and it was therefore necessary to exclude these compounds from the QSAR analysis for both the ketone and *gem*-diol equations.

We analyzed the substituent effects on the inhibition for set of substituted phenyl analogues listed in Table 3, using Hansch–Fujita method.[35] For mono-substituted compounds (**50**–**72**), we derived eq. 8. We do not report separate equations for the ketone and *gem*-diol inhibitors for eqs 8 and 9 because these equations are extremely similar and only differ in their constant values. Therefore only ketone data are shown.

$$\begin{aligned} pIC_{50} =& 0.787(\pm 0.340)\log P - 1.199(\pm 0.836)\sigma \\ & + 3.718(\pm 1.053) \\ n = 23 \quad & s = 0.550 \quad r^2 = 0.579 \\ F(2,20) = 13.793 \quad & p < 0.001 \end{aligned} \tag{8}$$

As shown in eq. 8, the inclusion of the electronic parameter σ provided a significant result. We therefore included the summation values for multiple substitutions (**73**–**86**) as shown in eq. 9.

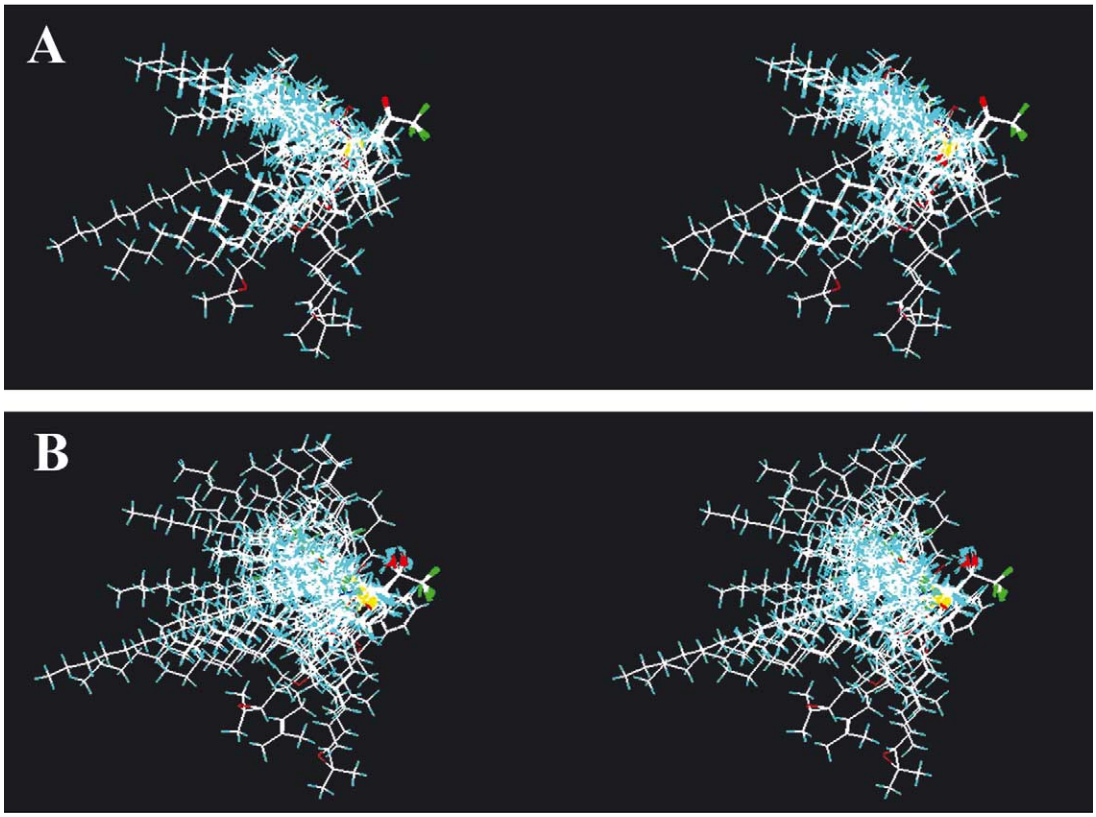

Figure 5. Stereoview of the superposition of all 109 compounds used in CoMFA analysis with both the ketone (A) and *gem*-diol (B) conformations.

$$\begin{aligned} pIC_{50} &= 0.999(\pm 0.291)\log P - 0.670(\pm 0.541)\Sigma\sigma \\ &\quad + 3.216(\pm 0.970) \\ n &= 37 \quad s = 0.653 \quad r^2 = 0.590 \\ F(2, 34) &= 24.386 \quad p < 0.001 \end{aligned} \tag{9}$$

Of particular interest in eqs 8 and 9 is the observation that the squared term of log P was not significant (as opposed to eqs 1–7). TFK-containing JHE inhibitors usually provide a parabolic relationship between activity and log P.[12] However, since the log P values for all of the substituted phenyl analogues were less than the optimum log P (≈ 6.2), it is reasonable that the squared term was not significant.

3-D QSAR with CoMFA

CoMFA analyses were performed to explore the steric and electronic parameters that contributed to biological activity and to determine if either played a role in determining the ketone hydration state. A total of 12 compounds (out of the original set of 109 inhibitors) were excluded to derive the optimal classical QSAR equations discussed above (eq. 7). We therefore first examined the 3-D QSAR of this reduced data set in equation 10 using the superposed compounds shown in Figure 5. In eqs 10–12, the *gem*-diol did not provide significant correlations as determined by the low cross-validated correlation coefficient ($q^2 < 0.3$). Subsequently, no *gem*-diol equations are shown and eqs 10–12 are for the ketone only.

$$\begin{aligned} pIC_{50} &= 4.483 + [\text{CoMFA term}] \\ n &= 97 \quad s = 0.368 \quad r^2 = 0.913 \\ m &= 7 \quad (q^2 = 0.487, \ \text{SD} = 0.896) \\ &(\text{Steric: } 69.7\%; \ \text{Electrostatic: } 30.3\%) \end{aligned} \tag{10}$$

We then examined the activity of the entire data set and derived eq. 11.

$$\begin{aligned} pIC_{50} &= 4.702 + [\text{CoMFA term}] \\ n &= 109 \quad s = 0.481 \quad r^2 = 0.884 \\ m &= 6 \quad (q^2 = 0.422, \ \text{SD} = 1.073) \\ &(\text{Steric: } 69.2\%; \ \text{Electrostatic: } 30.8\%) \end{aligned} \tag{11}$$

However, since the deviation of compound **105** was quite large (>2 log units), this compound was omitted to derive eq. 12.

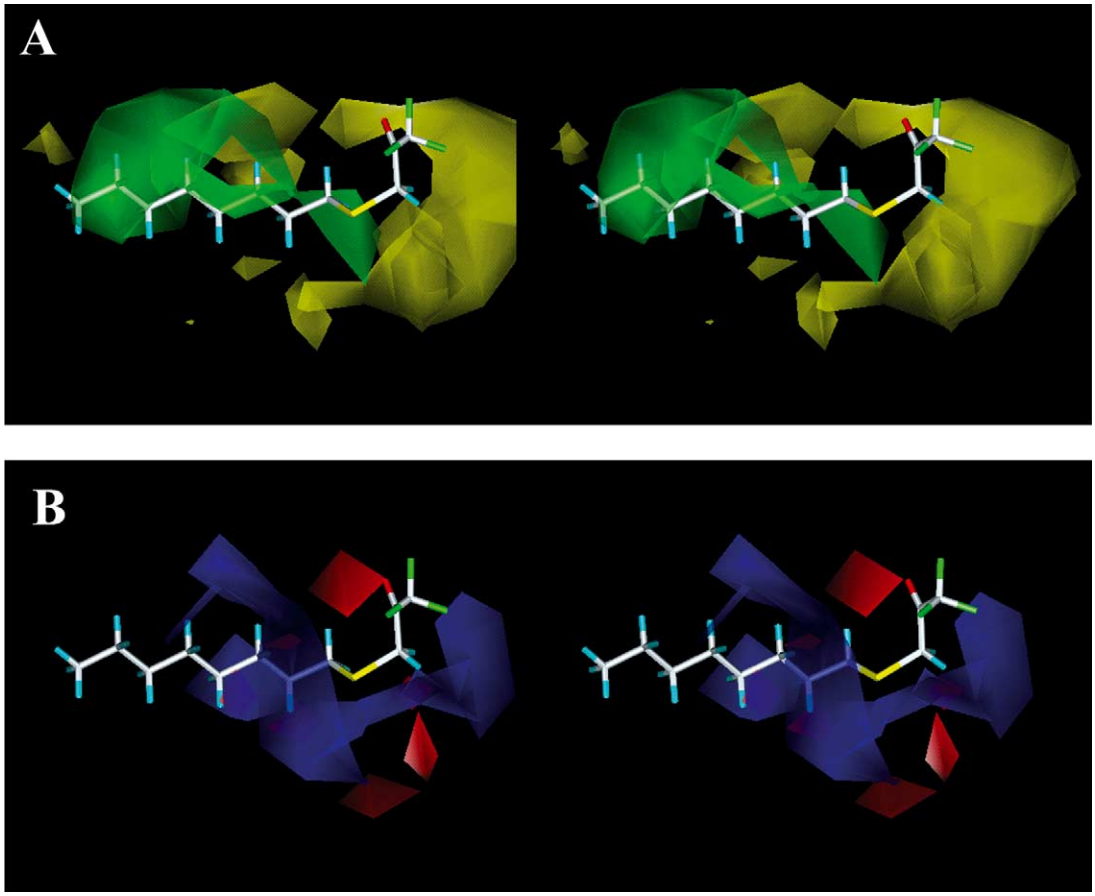

Figure 6. Stereoviews of CoMFA analysis according to eq 12, shown with 3-octylthio-1,1,1-trifluoropropan-2-one (compound **30**, OTFP). The contours are shown to surround regions where a higher steric bulk increases (green) or decreases (yellow) the inhibition (A) or where a positive (blue) or a negative (red) electrostatic potential increases the inhibition (B).

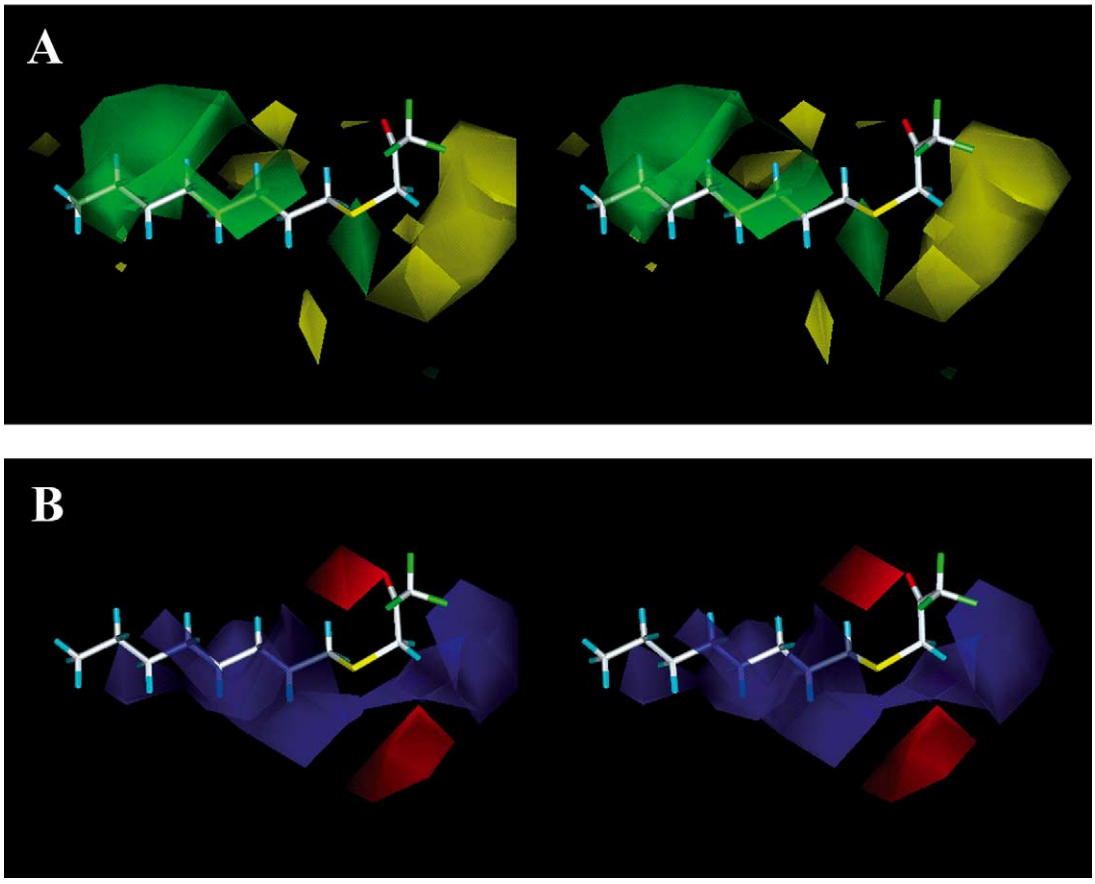

Figure 7. Stereoviews of CoMFA analysis according to eq 13, which includes the hydrophobicity descriptors log P and $(\log P)^2$. Figures are shown with 3-octylthio-1,1,1-trifluoropropan-2-one (compound **30**, OTFP). The contours are shown to surround regions where a higher steric bulk increases (green) or decreases (yellow) the inhibition (A) or where a positive (blue) or a

$$\begin{aligned} pIC_{50} &= 4.751 + [\text{COMFA term}] \\ n &= 108 \quad s = 0.465 \quad r^2 = 0.889 \\ m &= 6 \quad (q^2 = 0.412, \ \text{SD} = 1.068) \\ &(\text{Steric: } 68.9\%; \ \text{Electrostatic: } 31.1\%) \end{aligned} \tag{12}$$

Given the importance of the log P and $(\log P)^2$ terms in the classical QSAR analyses, they were added into the CoMFA equations for both the ketone and *gem*-diol. Eq 13 was generated for the ketone.

$$\begin{aligned} pIC_{50} &= 3.487 + 1.091 \ \log P - 0.091 \\ &\quad \times (\log P)^2 \\ &+ [\text{CoMFA term}] \\ n &= 108 \quad s = 0.441 \quad r^2 = 0.901 \\ m &= 7 \quad (q^2 = 0.500, \ \text{SD} = 0.990) \\ &[\text{Steric: } 45.1\%; \ \text{Electrostatic: } 25.6\%; \ \log P \\ &15.8\%; \ (\log P)^2\text{: } 13.4\%] \end{aligned} \tag{13}$$

Inclusion of the log P terms slightly improved the ketone equation (eq. 13 vs 12). The cross-validated q^2 value increased and the sum of squares deviation decreased. The equation for the *gem*-diol inhibitors was significantly improved upon the addition of the log P terms ($q^2 = 0.506$); however it was necessary to increase the number of components to achieve a meaningful result ($m = 8$). The *gem*-diol equation therefore required an extra component to generate the same q^2 value as the ketone equation ($m = 7$). This result is in agreement with other QSAR analyses showing that the ketone consistently provided improved correlations over the *gem*-diol.

Contour maps of eqs 12 and 13 were similar, but differed in some key areas as shown in Figures 6 and 7. The contour maps generated from eqs 10–12 were essentially identical and no differences in either steric or electronic fields could be extracted. Those contour maps are therefore not displayed. Eq 13 was used as the final CoMFA equation as it predicted experimental IC_{50} values better than all other CoMFA equations (including eq. 12). Table 7 lists the predicted values of all 109 compounds by eq. 13 and this relationship is shown graphically in Figure 8.

The steric fields shown in Figures 6A and 7A agree very well with what is currently known about the structure of JHE. There is a region of unfavorable steric activity along the backbone of the inhibitor, indicating that any large substitutions would be detrimental for activity. This observation agrees well with the homology model

Table 7. CoMFA predicted pIC_{50} values for ketone inhibitors using eq 13

No.	Obsvd[a]	Calcd[b]	Dev[c]	No.	Obsvd[a]	Calcd[b]	Dev[c]	No.	Obsvd[a]	Calcd[b]	Dev[c]
1	3.66	4.12	−0.46	**38**	7.82	7.58	0.24	**75**	7.70	8.01	−0.31
2	4.17	4.55	−0.38	**39**	7.16	7.98	−0.82	**76**	6.04	6.92	−0.88
3	5.17	5.10	0.07	**40**	7.35	7.32	0.03	**77**	6.77	6.48	0.29
4	6.66	6.14	0.52	**41**	6.40	6.93	−0.53	**78**	6.92	6.46	0.46
5	7.00	6.47	0.53	**42**	6.20	6.48	−0.28	**79**	7.96	7.85	0.11
6	5.41	5.87	−0.46	**43**	6.30	6.03	0.27	**80**	5.74	6.62	−0.88
7	5.14	5.72	−0.58	**44**	5.01	4.86	0.15	**81**	8.52	8.24	0.28
8	4.85	4.97	−0.12	**45**	5.28	5.25	0.03	**82**	7.89	8.44	−0.55
9	3.04	3.41	−0.37	**46**	8.35	8.32	0.03	**83**	7.49	7.11	0.38
10	4.15	3.78	0.37	**47**	8.12	8.15	−0.03	**84**	5.92	5.49	0.43
11	6.52	6.59	−0.07	**48**	8.51	8.33	0.18	**85**	7.80	7.00	0.80
12	6.70	6.62	0.08	**49**	8.49	8.61	−0.12	**86**	4.96	5.80	−0.84
13	3.30	3.02	0.28	**50**	5.06	5.34	−0.28	**87**	4.82	4.60	0.22
14	5.14	5.21	−0.07	**51**	5.68	5.83	−0.15	**88**	5.18	4.81	0.37
15	4.10	4.99	−0.89	**52**	6.17	6.11	0.06	**89**	5.34	4.96	0.38
16	6.06	5.57	0.49	**53**	5.37	5.81	−0.44	**90**	4.90	4.73	0.17
17	5.49	4.69	0.80	**54**	5.54	6.14	−0.60	**91**	5.10	5.14	−0.04
18	6.40	6.20	0.20	**55**	6.47	6.51	−0.04	**92**	5.20	5.30	−0.10
19	7.24	7.33	−0.09	**56**	5.70	5.49	0.21	**93**	5.80	5.57	0.23
20	7.57	7.88	−0.31	**57**	5.15	4.68	0.47	**94**	5.49	5.99	−0.50
21	8.00	7.89	0.11	**58**	6.66	6.61	0.05	**95**	6.77	6.88	−0.11
22	5.27	5.21	0.06	**59**	7.52	7.34	0.18	**96**	7.37	7.37	0.00
23	5.82	5.68	0.14	**60**	6.40	6.50	−0.10	**97**	4.21	4.59	−0.38
24	6.11	6.59	−0.48	**61**	6.06	6.85	−0.79	**98**	7.64	6.76	0.88
25	5.30	4.96	0.34	**62**	5.60	6.10	−0.50	**99**	3.98	4.48	−0.50
26	5.80	5.76	0.04	**63**	6.89	6.84	0.05	**100**	6.83	6.73	0.10
27	5.60	5.90	−0.30	**64**	5.89	5.93	−0.04	**101**	6.90	7.17	−0.27
28	7.51	7.91	−0.40	**65**	5.08	5.45	−0.37	**102**	7.36	7.38	−0.02
29	8.09	7.43	0.66	**66**	5.89	6.07	−0.18	**103**	7.21	7.03	0.18
30	8.62	8.23	0.39	**67**	6.39	6.28	0.11	**104**	6.31	6.13	0.18
31	7.98	8.07	−0.09	**68**	6.96	6.75	0.21	**105**	9.06[d]	6.83	2.21
32	8.43	8.38	0.05	**69**	8.12	7.86	0.26	**106**	5.32	5.75	−0.43
33	9.77	8.64	1.13	**70**	5.21	4.99	0.22	**107**	4.09	4.57	−0.48
34	7.70	7.15	0.55	**71**	5.89	6.18	−0.29	**108**	4.09	3.33	0.76
35	8.24	8.73	−0.49	**72**	7.05	7.08	−0.03	**109**	8.07	6.75	1.32
36	7.37	7.83	−0.46	**73**	7.64	7.35	0.29				
37	7.89	7.82	0.07	**74**	7.11	6.69	0.42				

[a]Observed pIC_{50} values taken from Székács,[12] except for compounds **100**–**104** which are from Kamita.[9]
[b]Calculated pIC_{50} values for ketone inhibitors using eq 13.
[c]Deviation in ketone inhibitor pIC_{50} values calculated with eq 13 from observed values.
[d]Not included in the final CoMFA (eq 13).

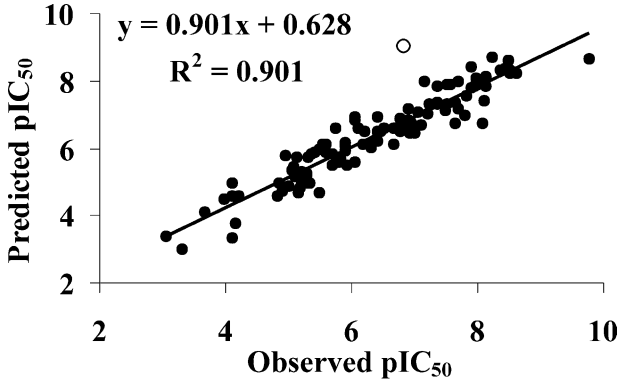

Figure 8. Graphical representation of observed pIC_{50} values versus pIC_{50} values calculated with eq 13 for 108 compounds. The clear circle is compound **105**, which was not included in the regression analysis.

for JHE showing a long narrow channel for the active site.[11] This field is more pronounced in the absence of hydrophobicity descriptors, showing that log P accounts for a large amount of the steric field observed in Figure 6A. There is also a series of small unfavorable fields surrounding the α position to the carbonyl that is more pronounced in Figures 7A than 6A. These fields are a function of the steric hindrance observed with compounds **105**–**109** in Table 6. Interestingly, the favorable activity of methyl substitution in the α or γ position is not shown in the CoMFA field in the absence of hydrophobic parameters. Only Figure 7A displays favorable steric activity in these positions. The main favorable steric field observed was located at approximately 7–8 atoms from the carbonyl. However this field becomes sterically unfavorable greater than 10 atoms from the carbonyl. This result most likely reflects the parabolic nature of the dependence of these compounds upon log P.

There was not a large difference in the electrostatic contour maps generated in the presence and absence of hydrophobicity descriptors. As shown in Figures 6B and 7B, negative electrostatic potentials are scattered around the β position. This is most likely a reflection of the high electron density and enhanced activity of both the sulfur-containing and unsaturated compounds. A small area of negative potential was also observed at the position δ to the carbonyl. This area of favorable activity could result from compounds **11**, **12**, **48**, and **49**, which all contain an olefin in this position. There is a large field of favorable positive electrostatic potential

surrounding the middle of the inhibitor backbone in both Figures 6B and 7B, however this field is more pronounced in Figure 7B. This favorable activity is novel and has not been reported in other studies. The physiochemical basis of these fields is questionable because none of the compounds used to build the CoMFA model contain the appropriate functional groups to generate positive fields.

Discussion

The study of enzyme inhibition mechanisms is useful for understanding biological pathways and determining the physiological role of an enzyme.[14] This is particularly important for esterases whose physiological role is still unclear. JHE is an excellent model for these studies since it is one of the few esterases that has a clear physiological function.[8] In addition, the enzyme preparations used in these studies, while not pure, do consist of primarily one enzyme.[36,37] Lastly, there is an extremely large body of literature dealing with JHE biochemistry and inhibition mechanism (see Kamita and references therein).[9] However, one of the few remaining facets still not understood about the TFK inhibition mechanism is the hydration state of the active form of the inhibitor as shown in Figure 2. We therefore used both classical and 3-D QSAR to compare the hydration state of the ketone and *gem*-diol forms in order to address the question 'What is the active form of the inhibitor?'.

Classical QSAR

For the classical QSAR analysis, we developed a series of equations for both forms of the inhibitor. This work was a continuation of studies performed by Székács.[12] They examined the classical QSAR of a number of TFK inhibitors; however, they failed to extend these QSAR relationships to a single equation for a range of compounds. We included 97 compounds in our final equation and found that log P was the most important descriptor of activity and described the majority of activity. Of particular interest is the necessity of including the $(\log P)^2$ term. This parabolic relationship indicates that there is an optimum log P value for enzyme inhibition, which is often observed for QSAR studies involving compounds penetrating through aqueous or lipid phases.[33] These results agree with published reports that have shown that the most potent JHE inhibitors contain functional groups that extend for 10–12 atoms beyond the ketone and inhibition potency falls off with longer chain length.[12]

The similarity of eqs 1A and 1B suggests that the effects of log P outweigh any potential contributions from the ketone hydration state for saturated aliphatics. Subsequently, any effects resulting from ketone hydration are overshadowed by inhibitor hydrophobicity. In other words, a fully hydrated compound will not be potent if it does not exceed a minimal hydrophobicity value. This observation has been substantiated by lack of inhibition activity for compounds such as hexafluoroacetone, which is fully hydrated in solution.[12,38] These results are not surprising given that multiple research groups have shown that JHE inhibitors require a large hydrophobic group to achieve maximum inhibition potency, with log P values similar to JH. However, as soon as we began substituting functional groups into the aliphatic chain, log P was no longer sufficient to describe all of the biological activity. We therefore included other indicator variables for the functional groups into the equations.

For eqs 2A and 2B, the ketone and *gem*-diol compounds provided slightly different equations showing that upon the consideration of additional parameters, the dominant effect of log P is lessened and the importance of hydration state increases. Eqs 3A and 3B were generated by excluding compounds **13** and **15** from eqs 2A and 2B. As with most QSAR studies, the compounds that are excluded provide a great deal of information on the limitations of the model. Compound **13** is a JH analogue that contains two epoxide moieties. The fact that this complex molecule could not be predicted by a simple QSAR equation is not surprising. Of more interest is the exclusion of compound **15**, an inhibitor containing an olefin with *Z* geometry. The olefin in JH contains *E* geometry and it has been shown that inhibitors containing *Z* olefin geometry have much less activity against JHE.[20] Linderman hypothesized that this is caused by geometric constraints in the active site. These effects were observed in the 3-D QSAR analysis and are discussed under *3-D QSAR and CoMFA analyses* below.

The sulfur containing compounds represent the largest portion of the data set for this study. The role of this sulfur atom has been the focus of many studies that have attempted to explain its role in increased inhibitor potency.[12,24,30,39] Eq 5 combined the I-S and I-triple terms, which are related in that they describe electron density and are used to model functional groups that contain a significant amount of π electrons. The inclusion of these terms in the classical QSAR equation is interesting from the standpoint that it potentially provides evidence of the inhibition mechanism. The sulfur atom was originally substituted for a methylene group to mimic the double bond of JH, thereby mimicking the natural substrate of JHE and subsequently providing a more potent inhibitor.[39] A sulfur atom has a large van der Waals radius (≈180 pm as opposed to 155 pm for carbon) and was considered to be a bioisoster of the olefin, mimicking the electron distribution.[12] However, inhibitors with a sulfur β to the carbonyl proved to be potent inhibitors of not only JHE, but other carboxylesterases as well.[16,40] Therefore the original hypothesis that the sulfur atom would serve as a bioisoster appears to be more complex than first proposed. Work by Wheelock suggested that this observation could be explained by contributions to the hydration state of the inhibitor.[24] However, this simple explanation probably does not account for all of the observed effects. It is likely that the sulfur or olefin is interacting with other aromatic residues in the active site of the enzyme through π-interactions.[41] In order to determine the role of moieties in the β position, it would be necessary to

have structural information such as a crystal structure or from docking studies with the JHE homology model.[11]

The similarity in eqs 4–6 for the ketone and the *gem*-diol forms of the inhibitors suggest that the descriptor for the sulfide compounds (I-S) was extremely important for describing inhibitor potency—perhaps more important than inhibitor hydration state. The inclusion of the sulfone and sulfoxide compounds in eq. 7 had essentially equal effects upon the ketone and *gem*-diol equations, with the ketone form still providing the stronger correlation. These compounds (**96**–**104**) are important for the QSAR analysis because they are fully hydrated both in the crystalline state as well as in aqueous and organic solutions.[16,24] An X-ray crystal structure analysis of thioether-containing compounds showed that the ketone was hydrated.[34,42] However, by ^{1}H NMR, ^{19}F NMR (in deuterated chloroform) and IR all thioether compounds consistently were in the ketone form (showing $<5\%$ hydrate).[16,24] Therefore, even though the sulfone and sulfoxide analogues are predominantly hydrated in activity assays, their biological activity is best described by their ketone form as evidenced in eq. 7B. This observation highly suggests that the ketone is in fact the active form of the inhibitor.

The exclusion of compounds **33** and **105**–**109** provide information on the limitations of this simple description of binding described in this study. The activity of sulfide compounds containing large steric groups in the α-position was 300–5000 times lower than their predicted values (**106**–**108**), but a methyl group enhanced the activity 30 times (**105**). The importance of the sulfur atom in activity is still unclear, however it has been hypothesized that it contributes to potency through the formation of hydrogen bonds to the hydrated ketone.[24] Large steric substitutions in the α position could interfere with this activity. However, this does not explain why a methyl substitution is favorable. It would be necessary to synthesize the nonthioether-containing analogues with substituents in this position to see if this effect holds constant as a means to determine the role of sulfur. Alternatively, steric interference could prevent the sulfur from accessing other amino acid residues in the active site of the enzyme (such as π-interactions).

Eqs 8 and 9 showed that electron donating groups enhanced activity, indicating that the electron density of the sulfur atom in the β position was increased by the electron donating property of the substituents. Therefore, attempts to design more potent inhibitors could focus on including multiple electron donating groups on the aromatic moieties. Given the role of log P in activity, it is important that the inhibitor contain a significant hydrophobic group. Examining compounds **87**, **94** and **95** shows that activity increases with the number of methylene substitutions between the phenyl ring and the sulfur atom. It is likely that a more potent inhibitor could be designed by maximizing the number of methylene groups (likely from six to eight groups, based upon the optimal log P value) and adding strong electron donating groups on the ring.

CoMFA analyses

CoMFA analyses were in agreement with classical QSAR analyses, showing that *gem*-diol models were statistically inferior to ketone models. In the absence of log P and $(\log P)^2$ descriptors, the *gem*-diol models were not statistically significant. Only the inclusion of both terms generated a significant equation, however that relied upon the use of an extremely large number of components ($m=8$). The inclusion of the log P parameters in the ketone CoMFA analysis had very little effect. The fact that the additional use of the hydrophobicity descriptor did not improve the correlations for the combined set is not surprising as there is multiple collinearity among the hydrophobicity parameter and the CoMFA field descriptors.[43] Subsequently, the hydrophobic component is already described by the CoMFA terms and does not require an additional hydrophobicity parameter. It is difficult to separate steric and hydrophobic effects as the two are often collinear. However eq. 13 shows that ≈20% of the steric effects observed in eq. 12 can be attributed to purely hydrophobic effects.

The superposition of all 109 inhibitors in Figure 5 illustrates the main limitation of the *gem*-diol inhibitors. Their PM3 optimized geometries resulted in a wide distribution of inhibitor structures that did not superpose well. This spread in inhibitor geometry most likely resulted in the poor statistics of all *gem*-diol models. The fact that the *gem*-diol inhibitors could not be significantly described by CoMFA without the use of log P suggests that the ketone is the active inhibitor. The steric contour map in Figures 6A and 7A essentially described the current range of steric limitations upon JHE inhibitors. Previous studies had already shown that optimal inhibitors should consist of 10∼12 atoms past the carbonyl and that minimal branching was preferred for potency. Interestingly, only the CoMFA study that included hydrophobic descriptors was able to detect the favorable effects of the methyl substitution in the α and γ position. This result suggests that separating out hydrophobic effects is important for examining subtle steric effects. These results confirm that any further synthesis of JHE inhibitors should confine chain length to 10∼12 atoms beyond the carbonyl (10.9–13.7 Å).

The electronic contour maps were not greatly different between the two CoMFA models as would be expected given that the models differ by the inclusion of hydrophobic parameters. Figures 6B and 7B show a large field of negative electropotential surrounding the β position, which is indicative of the favorable effects of the sulfur atom or the olefin. It has been suggested that the increased potency of sulfur is due to hydrogen bond formation with the hydrated ketone.[24] However, this negative field strongly points to the potential for groups in this position to interact with amino acid residues in the enzyme active site. These effects can only be elucidated with a JHE crystal structure. Another area of negative potential was observed 6∼7 carbons from the carbonyl carbon atom. This area represents an additional unexplored area for biological activity. These

areas of favorable negative potential are reflective of the inclusion of the I-S and I-triple terms in the classical QSAR analysis.

Another novel area for favorable activity is the positive field along the inhibitor backbone. This field was present in both CoMFA models, but was larger in Figure 7B. This activity has not been reported in previous work and could represent a novel site for inhibitor interactions with the enzyme. However, none of the compounds analyzed in this study contain the requisite functional groups to generate positive fields in these areas. This result has been observed in CoMFA analyses before and is attributed to the accumulated effects of polarization of carbon–hydrogen bonds.[44] Given that the majority of inhibitors used in this study consist of alkyl chains in this position, it is possible that carbon–hydrogen bond polarization could account for the observed positive fields. Further studies should explore different pharmacophores that could be placed in this position to take advantage of the positive field and test if the fields are truly favorable for activity or just an artifact of the CoMFA analyses.

Conclusion

In all of the classical QSAR equations, the ketone consistently provided improved correlations relative to the *gem*-diol. However the final equations for both the ketone (7A) and the corresponding *gem*-diol (7B) did an excellent job of describing activity for a wide range of compounds, with log P and $(\log P)^2$ being the most important parameters. It is difficult to determine conclusively from the classical QSAR analysis the form of the inhibitor that inhibits the enzyme. Analysis by 3-D QSAR also consistently provided statistically superior results with the ketone inhibitors versus the *gem*-diol. Only the inclusion of additional hydrophobicity parameters resulted in a significant 3-D QSAR equation for the *gem*-diol, further illustrating the importance of hydrophobic descriptors in the activity of these inhibitors. Neither of these analyses proves conclusively which form of the inhibitor is the active form, yet the constant superiority of the ketone equations over those of the *gem*-diol suggests that the ketone is the active form. It is unclear as to where the inhibitor undergoes dehydration before inhibition. All studies on these compounds show that potent inhibitors are hydrated in the aqueous phase. Therefore if the ketone is the active inhibitor, dehydration must occur at some point during the inhibition process. According to Figure 2, it is most likely step **D**, with the inhibitor dehydrating inside the enzyme. The protein microenvironment inside an enzyme represents a hydrophobic environment that could catalyze the release of water from the inhibitor. Following dehydration, it would be necessary for the water to diffuse out of the active site of the enzyme. The emission of water following inhibitor or substrate binding has been demonstrated for other enzymes.[45]

We have developed two different QSAR models for JHE inhibition that both suggest that the ketone is the active inhibitor. The CoMFA analyses have identified several novel potential sites in the enzyme that could be targeted for the development of new JHE inhibitors. Further work in this area will require a structural component in terms of either a crystal structure of JHE or homology model studies to determine the exact binding constraints of these inhibitors.

Experimental

The syntheses and inhibition potencies of all compounds were reported in previously published work.[9,12,16] Compounds **100**–**104** were originally reported by Wheelock.[16] However the IC_{50} values were determined using inhibitor dilutions prepared in DMF, which has been shown to affect inhibitor potency. In the work by Székács, all inhibitor dilutions were prepared in ethanol.[12] Kamita re-examined the IC_{50} values of compounds **100**–**104** in ethanol and found that they were different from those reported by Wheelock.[16] All IC_{50} values employed in this work were determined with inhibitor dilutions prepared in ethanol for consistency.

Acknowledgements

The authors thank Jim Sanborn and Åsa Wheelock for helpful critique of this manuscript. We are grateful to the Japanese Society for the Promotion of Science (JSPS) for an invitational post doctoral fellowship to support C.E.W. at Kyoto University. C.E.W. was also supported by a UC TSR&TP graduate fellowship and NIH Post Doctoral training grant T32 DK07355-22. This project received financial assistance from NIEHS grant ES02710, NIEHS Superfund Basic Research Program ES04699, and USDA grant 2001-35302-09919.

References and Notes

1. Ollis, D. L.; Cheah, E.; Cygler, M.; Dijkstra, B.; Frolow, F.; Franken, S. M.; Harel, M.; Remington, S. J.; Silman, I.; Schrag, J.; Sussman, J. L.; Verschueren, K. H. G.; Goldman, A. *Protein Eng*. **1992**, *5*, 197.
2. Satoh, T.; Hosokawa, M. *Annu. Rev. Pharmacol. Toxicol*. **1998**, *38*, 257.
3. Bodor, N.; Buchwald, P. *Med. Res. Rev*. **2000**, *20*, 58.
4. Casida, J. E.; Gammon, D. W.; Glickman, A. H.; Lawrence, L. J. *Annu. Rev. Pharmacol. Toxicol*. **1983**, *23*, 413.
5. Wallace, T. J.; Ghosh, S.; Grogan, W. M. *Am. J. Respir. Cell Mol. Biol*. **1999**, *20*, 1201.
6. Gupta, R. C.; Dettbarn, W. D. *Chem.-Biol. Interact*. **1993**, *87*, 295.
7. Quinn, D. M. *Chem. Rev*. **1987**, *87*, 955.
8. Abdel-Aal, Y. A. I.; Hammock, B. D. *Science* **1986**, *233*, 1073.
9. Kamita, S. G.; Hinton, A. C.; Wheelock, C. E.; Wogulis, M. D.; Wilson, D. K.; Wolf, N. M.; Stok, J. E.; Hock, B.; Hammock, B. D. *Insect Biochem. Molec. Biol*. (In press).
10. Riddiford, L. M. In Comprehensive Insect Physiology, Biochemistry, and Pharmacology vol. 8; Pergamon: New York, 1985; p 37.
11. Thomas, B. A.; Church, W. B.; Lane, T. R.; Hammock, B. D. *Proteins* **1999**, *34*, 184.

12. Székács, A.; Bordás, B.; Hammock, B. D. In *Rational Approaches to Structure, Activity, and Ecotoxicology of Agrochemicals*; Draber, W.; Fujita, T., eds. CRC: Boca Raton, FL, 1992; p 219.
13. Lienhard, G. E. *Science* **1973**, *180*, 149.
14. Segel, I. H. In *Biochemical Calculations*, 2nd ed.; John Wiley & Sons: New York, 1976.
15. Nair, H. K.; Lee, K.; Quinn, D. M. *J. Am. Chem. Soc.* **1993**, *115*, 9939.
16. Wheelock, C. E.; Severson, T. F.; Hammock, B. D. *Chem. Res. Tox.* **2001**, *14*, 1563.
17. Amour, A.; Reboud-Ravaux, M.; de Rosny, E.; Abouabdellah, A.; Begue, J. P.; Bonnet-Delpon, D.; Le Gall, M. *J. Pharm. Pharmacol.* **1998**, *50*, 593.
18. Boger, D. L.; Sato, H.; Lerner, A. E.; Austin, B. J.; Patterson, J. E.; Patricelli, M. P.; Cravatt, B. F. *Bioorganic Med. Chem. Let.* **1999**, *9*, 265.
19. Edwards, P. D.; Andisik, D. W.; Bryant, C. A.; Ewing, B.; Gomes, B.; Lewis, J. J.; Rakiewicz, D.; Steelman, G.; Strimpler, A.; Trainor, D. A.; Tuthill, P. A.; Mauger, R. C.; Veale, C. A.; Wildonger, R. A.; Williams, J. C.; Wolanin, D. J.; Zottola, M. *J. Med. Chem.* **1997**, *40*, 1876.
20. Linderman, R. J.; Upchurch, L.; Lonikar, M.; Venkatesh, K.; Roe, R. M. *Pestic. Biochem. Physiol.* **1989**, *35*, 291.
21. Linderman, R. J.; Leazer, J.; Venkatesh, K.; Roe, R. M. *Pestic. Biochem. Physiol.* **1987**, *29*, 266.
22. Roe, R. M.; Linderman, R. J.; Lonikar, M.; Venkatesh, K.; Abdel-Aal, Y. A. I.; Leazer, J.; Upchurch, L. *J. Agric. Food Chem.* **1990**, *38*, 1274.
23. Ward, V. K.; Bonning, B. C.; Huang, T.; Shiotsuki, T.; Griffeth, V. N.; Hammock, B. D. *Int. J. Biochem.* **1992**, *24*, 1933.
24. Wheelock, C. E.; Colvin, M. E.; Uemura, I.; Olmstead, M. M.; Nakagawa, Y.; Sanborn, J. R.; Jones, A. D.; Hammock, B. D. *J. Med. Chem.* **2002**, *45*, 5576.
25. Linderman, R. J.; Jamois, E. A.; Roe, R. M. In *Reviews in Pesticide Toxicology*; North Carolina State University: Raleigh, 1991; p 261.
26. Hammock, B. D.; Wing, K. D.; McLaughlin, J.; Lovell, V. M.; Sparks, T. C. *Pestic. Biochem. Physiol.* **1982**, *17*, 76.
27. Linderman, R. J.; Leazer, J.; Roe, R. M.; Venkatesh, K.; Selinsky, B. S.; London, R. E. *Pestic. Biochem. Phys.* **1988**, *31*, 187.
28. Gelb, M. H.; Svaren, J. P.; Abeles, R. H. *Biochem.* **1985**, *24*, 1813.
29. Christianson, D. W.; Lipscomb, W. N. *J. Am. Chem. Soc.* **1986**, *108*, 4998.
30. Roe, R. M.; Anspaugh, D. D.; Venkatesh, K.; Linderman, R. J.; Graves, D. M. *Arch. Insect Biochem. Physiol.* **1997**, *36*, 165.
31. Asao, M.; Shimizu, R.; Nakao, K.; Fujita, T. *QREG*, 2.05 ed.; Chemistry Program Exchange: Kyoto, Japan.
32. Hansch, C. *ClogP*, 4.0 ed.; BioByte: Claremont, CA, USA.
33. Hansch, C.; Leo, A.; Haekman, D. In *Exploring QSAR: Hydrophobic, electronic and steric constants*. American Chemical Society: Washington, DC, USA, 1995; p 584.
34. Olmstead, M. M.; Musker, W. K.; Hammock, B. D. *Acta Crystallogr.* **1987**, *C43*, 1726.
35. Fujita, T.; Hansch, C. *J. Med. Chem.* **1967**, *10*, 991.
36. Sparks, T.; Hammock, B. *J. Insect. Physiol.* **1979**, *25*, 551.
37. Rudnicka, M.; Hammock, B. *Insect Biochem.* **1981**, *11*, 437.
38. Guthrie, J. P. *Can. J. Chem.* **1975**, *53*, 898.
39. Hammock, B. D.; Abdel-Aal, A. I.; Mullin, C. A.; Hanzlik, T. N.; Roe, R. M. *Pestic. Biochem. Phys.* **1984**, *22*, 209.
40. Shiotsuki, T.; Huang, T. L.; Hammock, B. D. *J. Pestic. Sci.* **1994**, *19*, 321.
41. Morgan, R. S.; McAdon, J. M. *Int. J. Peptide Protein Res.* **1980**, *15*, 177.
42. Székács, A.; Halarnkar, P. P.; Olmstead, M. M.; Prag, K. A.; Hammock, B. D. *Chem. Res. Toxicol.* **1990**, *3*, 325.
43. Akamatsu, M.; Nishimura, K.; Osabe, H.; Ueno, T.; Fujita, T. *Pestic. Biochem. Physiol.* **1994**, *48*, 15.
44. Avery, M. A.; Alvim-Gaston, M.; Rodrigues, C. R.; Barreiro, E. J.; Cohen, F. E.; Sabnis, Y. A.; Woolfrey, J. R. *J. Med. Chem.* **2002**, *45*, 292.
45. Davydov, D. R.; Hui Bon Hoa, G.; Peterson, J. A. *Biochemistry* **1999**, *38*, 751.